

This discussion paper is/has been under review for the journal *Climate of the Past* (CP).
Please refer to the corresponding final paper in CP if available.

Palaeogeographic controls on climate and proxy interpretation

D. J. Lunt¹, A. Farnsworth¹, C. Loptson¹, G. L. Foster², P. Markwick³,
C. L. O'Brien^{4,5}, R. D. Pancost⁶, S. A. Robinson⁴, and N. Wrobel³

¹School of Geographical Sciences, and Cabot Institute, University of Bristol, Bristol, BS8 1SS, UK

²Ocean and Earth Science, University of Southampton, and National Oceanography Centre, Southampton, SO14 3ZH, UK

³Getech Plc, Leeds, LS8 2LJ, UK

⁴Department of Earth Sciences, University of Oxford, Oxford, OX1 3AN, UK

⁵Department of Geology and Geophysics, Yale University, New Haven, CT 06511, USA

⁶School of Chemistry, and Cabot Institute, University of Bristol, Bristol, BS8 1TS, UK

Received: 16 November 2015 – Accepted: 1 December 2015 – Published: 14 December 2015

Correspondence to: D. J. Lunt (d.j.lunt@bristol.ac.uk)

Published by Copernicus Publications on behalf of the European Geosciences Union.

Palaeogeographic controls on the climate system

D. J. Lunt et al.

Title Page

Abstract

Introduction

Conclusions

References

Tables

Figures



Back

Close

Full Screen / Esc

Printer-friendly Version

Interactive Discussion



Abstract

During the period from approximately 150 to 35 million years ago, the Cretaceous–Paleocene–Eocene (CPE), the Earth was in a “greenhouse” state with little or no ice at either pole. It was also a period of considerable global change, from the warmest periods of the mid Cretaceous, to the threshold of icehouse conditions at the end of the Eocene. However, the relative contribution of palaeogeographic change, solar change, and carbon cycle change to these climatic variations is unknown. Here, making use of recent advances in computing power, and a set of unique palaeogeographic maps, we carry out an ensemble of 19 General Circulation Model simulations covering this period, one simulation per stratigraphic stage. By maintaining atmospheric CO₂ concentration constant across the simulations, we are able to identify the contribution from palaeogeographic and solar forcing to global change across the CPE, and explore the underlying mechanisms. We find that global mean surface temperature is remarkably constant across the simulations, resulting from a cancellation of opposing trends from solar and paleogeographic change. However, there are significant modelled variations on a regional scale. The stratigraphic stage–stage transitions which exhibit greatest climatic change are associated with transitions in the mode of ocean circulation, themselves often associated with changes in ocean gateways, and amplified by feedbacks related to emissivity and albedo. Our results also have implications for the interpretation of single-site palaeo proxy records. In particular, our results allow the non-CO₂ (i.e. palaeogeographic and solar constant) components of proxy records to be removed, leaving a more global component associated with carbon cycle change. This “adjustment factor” is illustrated for 7 key sites in the CPE, and applied to proxy data from Falkland Plateau, and we provide data so that similar adjustments can be made to any site and for any time period within the CPE.

Palaeogeographic controls on the climate system

D. J. Lunt et al.

[Title Page](#)

[Abstract](#)

[Introduction](#)

[Conclusions](#)

[References](#)

[Tables](#)

[Figures](#)



[Back](#)

[Close](#)

[Full Screen / Esc](#)

[Printer-friendly Version](#)

[Interactive Discussion](#)



1 Introduction

Over the last 150 million years, the climate of the Earth has experienced change across a broad range of timescales, from geological (10's of millions of years), to orbital 10's–100's of thousands of years), to millennial, to decadal.

Variability on timescales from geological to orbital has been characterised by measurements of the isotopic composition of oxygen in the calcium carbonate of benthic foraminifera ($\delta^{18}\text{O}_{\text{benthic}}$, e.g. Friedrich et al. (2012); Cramer et al. (2009), Fig. 1); this indicates, in the broadest sense, a long-term cooling (and increasing ice volume) trend from the mid Cretaceous (~ 100 million years ago, 100 Ma) to the modern. Imprinted on this general cooling are several shorter geological-timescale variations such as cooling through the Paleocene (65 to 55 Ma), and sustained warmings in the early Eocene (55 to 50 Ma) and middle Miocene (17 to 15 Ma). The $\delta^{18}\text{O}_{\text{benthic}}$ record also shows evidence for orbital scale variability in icehouse periods (for example Quaternary glacial–interglacial cycles, from around ~ 2 Ma) and greenhouse periods (for example Paleogene hyperthermals, ~ 55 Ma), and other events occurring on sub-geological timescales, such as the Eocene–Oligocene boundary (34 Ma) and Cretaceous Oceanic Anoxic Events (OAEs, ~ 100 Ma).

A methodology for reconstructing the global-mean surface temperature of the past ~ 65 million years has been developed by Hansen et al. (2013), making assumptions about the relationship between $\delta^{18}\text{O}_{\text{benthic}}$ and deep ocean temperature, and between deep ocean temperature and surface temperature (Fig. 1). The assumptions mean that the absolute values of temperature need to be treated with considerable caution, but the record indicates global mean surface temperatures of $\sim 25^\circ\text{C}$ in the Paleocene, peaking at over 28°C in the early Eocene. From the early Eocene to the present day, there is a general cooling trend, with temperatures decreasing to $\sim 24^\circ\text{C}$ degrees by the late Eocene. Today, global mean surface temperature is close to 15°C .

Although it has long been thought that greenhouse gas concentrations are the primary cause of Cretaceous and Eocene warmth (Barron and Washington, 1984; Barron

Palaeogeographic controls on the climate system

D. J. Lunt et al.

Title Page

Abstract

Introduction

Conclusions

References

Tables

Figures



Back

Close

Full Screen / Esc

Printer-friendly Version

Interactive Discussion



et al., 1995), the reasons for variability within this period are currently largely unknown. Possible candidates for the forcing on the Earth system on these timescales include changes in solar forcing, direct tectonic forcing, and greenhouse gas forcing (most likely CO₂) through changes in the carbon cycle, or some combination of these.

The solar forcing is related to a increase in solar constant, resulting from an increasing luminosity of the sun over 10's of millions of years. This itself is due to continued nuclear fusion in the core of the Sun, converting hydrogen into helium, reducing the core's density (Fig. 2, Gough, 1981). As a result, the core contracts and temperature increases. The increase in luminosity is a consequence of this core temperature increase. According to the solar model of Gough (1981), the solar constant increases nearly linearly from ~ 1348 W m⁻² at 150 Ma to 1365 W m⁻² for the modern.

Also over the timescales of tens of millions of years, plate tectonics has led to major changes in the position and configuration of the continents, and bathymetric and topographic depths and heights. These changes can have a direct effect on climate, for example through changing the global distribution of low-albedo (ocean) vs. high-albedo (land) surfaces (e.g. Barron et al., 1980), and/or changing ocean gateways leading to modified ocean circulation (e.g. Zhang et al., 2011), and/or topography modifying the area of land above the snowline (e.g. Foster et al., 2010) or atmospheric circulation (e.g. Ruddiman and Kutzbach, 1989). Palaeogeographical reconstructions for certain periods in Earth's history exist (e.g. Scotese, 2001), but not always at high temporal resolution, nor in a form which can readily be implemented into a climate model. In Sect. 2.1 we present a new set of palaeogeographical reconstructions which span the Cretaceous–Paleocene–Eocene, from approximately 150 to 35 Ma (Fig. S1 in the Supplement).

The greenhouse gas forcing could itself be indirectly related to tectonic changes, through changes in the balance of sources (e.g. volcanism) and/or sinks (e.g. weathering of silicate rocks, Raymo et al., 1988) of CO₂, or other greenhouse gases, and/or changes to the sizes of the relevant reservoirs (e.g. due to changes in the residence time of carbon in the ocean due to changes in ocean circulation, Lauderdale et al.,

Palaeogeographic controls on the climate system

D. J. Lunt et al.

Title Page

Abstract

Introduction

Conclusions

References

Tables

Figures



Back

Close

Full Screen / Esc

Printer-friendly Version

Interactive Discussion



Palaeogeographic controls on the climate system

D. J. Lunt et al.

[Title Page](#)[Abstract](#)[Introduction](#)[Conclusions](#)[References](#)[Tables](#)[Figures](#)[Back](#)[Close](#)[Full Screen / Esc](#)[Printer-friendly Version](#)[Interactive Discussion](#)

2013, themselves driven ultimately by tectonic changes. In addition, greenhouse gases will also likely be modified in response to climate changes caused by the solar or direct tectonic forcing. Efforts have been made to reconstruct the history of CO₂ over geological timescales (e.g. see compilation in Fig. 3, Honisch et al., 2012). However, CO₂ proxies are still associated with relatively large uncertainties, despite currently undergoing a period of rapid development (e.g. Zhang et al., 2013; Franks et al., 2014; Martinez-Boti et al., 2015).

Disentangling these various forcings on long-term climate evolution is a key challenge. Previous work has often been in a modelling framework, and has focused on either the role of palaeogeography across time (e.g. Donnadieu et al., 2006), or the role of CO₂ for a particular period (e.g. Caballero and Huber, 2013).

Given the uncertainties in CO₂ concentration and the carbon cycle, and to avoid complications of the feedbacks associated with continental ice, in this paper we focus on the direct role of palaeogeography and solar forcing on controlling the greenhouse climates from the earliest Cretaceous to the end of the Eocene (Cretaceous–Paleocene–Eocene, CPE). This also allows us to provide an “adjustment factor” for palaeo proxy records, which accounts for the non-CO₂ component of climate change (see Sect. 3.4).

The very first attempts to model time periods within the CPE were carried out in the laboratory, with rotating water tanks covered with moulded foam representing palaeogeography, and jets of compressed air simulating wind stress (Luyendyk et al., 1972). Several early numerical modelling studies also focused on the ocean circulation, and in particular the flow regime through the Tethys seaway (e.g. Barron and Peterson, 1990). The relative importance of paleogeography vs. surface albedo vs. greenhouse gases in warm paleoclimates were examined using what would now be considered low resolution GCMs (Barron and Washington, 1984; Barron et al., 1995) or using energy-balance models (Barron et al., 1980). These indicated that CO₂ was likely the primary driver of Cretaceous and Eocene warmth. The majority of modelling work since then has focused on the periods of maximum warmth, i.e. during the mid Cretaceous (e.g. Sellwood et al., 1994; Poulsen et al., 2001, 2003; Zhou et al., 2012) or Early Eocene

Palaeogeographic controls on the climate system

D. J. Lunt et al.

Title Page

Abstract

Introduction

Conclusions

References

Tables

Figures



Back

Close

Full Screen / Esc

Printer-friendly Version

Interactive Discussion



(e.g. Huber and Caballero, 2011); see summary in Lunt et al. (2012), or transient hyperthermals such as the PETM (e.g. Winguth et al., 2010). Several studies have addressed issues of model–data comparisons, including the interpretation of oxygen isotope proxies in both continental and oceanic proxies (e.g. Poulsen et al., 2007; Zhou et al., 2008), or uncertainties in Mg/Ca calibrations (e.g. Bice et al., 2003, 2006). Recently, it has been argued that if these uncertainties, and other issues such as seasonality of the proxies, are taken into account, then some models can simulate the climate of the early Eocene consistently with the data (Lunt et al., 2012).

Although no previous study has explored the role of varying palaeogeography throughout the CPE as we do here, several previous modelling studies are worth noting, which carried out sensitivity studies to palaeogeography with a more limited scope. Poulsen et al. (2001, 2003) carried out model simulations under two different Cretaceous palaeogeographies, representing conditions before and after the separation of the African and South American continents to form the Atlantic. They found that continental positions strongly influenced ocean circulation, in particular regions of deep water formation. Bice and Marotzke (2002) examined the role of ocean gateways in the Eocene, and found that the configuration of polar seaways affected the sensitivity of climate to hydrological forcing, through changes in ocean overturning. Spicer et al. (2008) used three Cretaceous palaeogeographies, and compared a number of model simulations with data from the Cretaceous Siberian continental interior, but the sensitivity studies were not consistent across the time periods. Donnadieu et al. (2006) also examined three palaeogeographies through the Cretaceous, using the FOAM model coupled to a slab ocean. They focused on the influence of continentality on seasonality, but noted that changing palaeogeography alone could give a $\sim 4^{\circ}\text{C}$ global-mean warming at a constant CO_2 level.

Our work presented here builds on these and other previous studies, but represents an advance because (a) new palaeogeographic maps of this time period have become available, which improve on previous representations in terms of both accuracy and temporal resolution (see Sect. 2.1) and (b) increases in available computing power

2.3 Solar forcing

The insolation at the top of the atmosphere (Total Solar Irradiance, TSI) for each Stage was calculated following Gough (1981), and is shown in Fig. 2. The evolution of TSI is very similar to that from Caldeira and Kasting (1992), also shown in Fig. 2.

2.4 Model description

The simulations described in this paper are all carried out using the UK Met Office coupled ocean–atmosphere general circulation model HadCM3L version 4.5. HadCM3L has been used in several palaeoclimate studies for different geological periods including the early Eocene (e.g. Lunt et al., 2010; Loptson et al., 2014) and the late Miocene (e.g. Bradshaw et al., 2012). The resolution of the model is 3.75° in longitude by 2.5° in latitude, with 19 vertical levels in the atmosphere and 20 vertical levels the ocean. The HadCM3L model is very similar to HadCM3, a description of which can be found in Gordon et al. (2000), but HadCM3L has a lower horizontal resolution in the ocean ($3.75^\circ \times 2.5^\circ$ compared with $1.25^\circ \times 1.25^\circ$).

In addition, HadCM3L is coupled to the dynamic global vegetation model TRIFFID (Top-down Representation of Interactive Foliage and Flora Including Dynamics) (Cox et al., 2001) via the land surface scheme MOSES 2.1 (Cox et al., 1999). TRIFFID calculates the fraction of each gridcell occupied by each of five plant functional types: broadleaf trees, needleleaf trees, C_3 grasses, C_4 grasses and shrubs. Although TRIFFID simulates modern Plant Functional Types, it has been argued that such a model can provide the first order signal from vegetation feedbacks through the last 250 million years (Donnadieu et al., 2009; Zhou et al., 2012).

The overall model, HadCM3L-MOSES2.1-TRIFFID is identical to that used in Loptson et al. (2014).

Title Page

Abstract

Introduction

Conclusions

References

Tables

Figures



Back

Close

Full Screen / Esc

Printer-friendly Version

Interactive Discussion



2.5 Simulation description

All simulations have undergone the same spin-up procedure, totaling 1422 years, with the same initial conditions and boundary conditions, with the exception of solar constant and palaeogeography (as discussed in Sects. 2.3 and 2.1). The ocean is initialised as stationary, with a zonal mean temperature structure given by an idealised cosine function of latitude ($\frac{21-z}{20} 22 \cos(\phi) + 10$, where ϕ is latitude and z is the model vertical level from 1 at the ocean surface to 20 at a depth of ~ 5200 m), and a constant salinity of 35 ppt. The atmosphere is initialised from an arbitrary atmospheric state from a previous preindustrial simulation. Land-surface initial conditions (e.g. soil moisture, soil temperature) are globally homogeneous.

The spinup procedure consists of four “Phases”. The first 50 years (Phase 1) of each simulation are run with an atmospheric CO₂ concentration of $1 \times \text{PI}$, and with global vegetation fixed as bare soil. For the next 319 years (Phase 2), the atmospheric CO₂ is increased to $4 \times \text{PI}$, the TRIFFID vegetation component of the model is turned on, and the vertical structure of atmospheric ozone is diagnosed from the modelled troposphere height as opposed to from a prescribed field (in order to avoid a runaway greenhouse encountered in previous high-CO₂ simulations with fixed ozone distributions). Phase 3 consists of 53 years of simulation in which prescribed lakes and glaciers are added to the model (see Sect. 2.1). In the first three Phases, the ocean dynamics are simplified to enhance stability, by imposing a purely baroclinic ocean circulation in which the vertically integrated flow is zero. The final phase, Phase 4, consists of a final 1000 years in which both the baroclinic and barotropic ocean dynamics are turned on, giving a total of 1422 years of simulation. The barotropic streamfunction calculation requires islands to be defined manually – these are shown in Fig. S4 in the Supplement. In addition, to maintain model stability, for some Stages additional smoothing/flattening of the topography was required at the beginning of Phase 4.

The details of the simulations are summarised in Table 1.

CPD

11, 5683–5725, 2015

Palaeogeographic controls on the climate system

D. J. Lunt et al.

Title Page

Abstract

Introduction

Conclusions

References

Tables

Figures



Back

Close

Full Screen / Esc

Printer-friendly Version

Interactive Discussion



the first-order response seen in the data during periods when atmospheric CO₂ is better constrained; however, these will not be discussed in this paper; instead, they will be presented in detail in future publications.

It is clear that for the Paleocene and Eocene, there is much less variability and trend in the modelled simulations than suggested by the proxy surface temperature record. Even accounting for the considerable uncertainties in the proxy record, this implies that the majority of the variability in the proxy data is caused by forcings which are not included in the model simulations. The most likely missing forcing is greenhouse gas forcing, probably primarily CO₂, caused by changes in the carbon cycle on multi-million year timescales.

The Hansen et al. (2013) record implies warmer temperatures than given by our results. Our latest Eocene simulation has a similar temperature to that of the earliest Oligocene in the Hansen et al. (2013) record. If both the model and proxy record are correct, then this implies that the earliest Oligocene had an atmospheric CO₂ concentration of about 1120 ppmv. However this is higher than the values recently reconstructed from CO₂ proxies (Pearson et al., 2009; Pagani et al., 2011), which imply Oligocene CO₂ concentrations closer to 600 ppmv. Indeed, in principle it would be possible to obtain a perfect match between the modelled and observed global means, by choosing an appropriate CO₂ level in the model, thereby generating a model-derived CO₂ record, for comparison with other proxy CO₂ records such as Beerling and Royer (2011). However, given the considerable uncertainties in the Hansen et al. (2013) record, we consider that this would be of little value. Instead, we await the development of more long-duration single-site SST proxy records, across a wide geographical range, and with full consideration of uncertainties, with which to compare our simulations.

Whilst the variability in mean annual temperature between our simulations is less than the available climate records imply, there is some variability present. In particular there is a long-term warming trend through the CPE. The trend is 0.0043 °C per million years (correlation coefficient of 0.42). There is a maximum scatter around this trend of

Palaeogeographic controls on the climate system

D. J. Lunt et al.

Title Page

Abstract

Introduction

Conclusions

References

Tables

Figures



Back

Close

Full Screen / Esc

Printer-friendly Version

Interactive Discussion



of the change in solar constant through the simulations, this is best expressed in terms of the temperature anomaly in each Stage, relative to the previous Stage (Fig. 6; see also Fig. S5 in the Supplement for the absolute temperature of each Stage, and Fig. S6 in the Supplement for the temperature anomaly of each Stage relative to the mean of all Stages). Looking Stage-to-Stage also minimises the effects of the changing land–sea contrast due to continental plate movements.

The response of the system to the palaeogeographic forcing is highly complex, mediated by positive and negative feedbacks. Here we use a number of approaches to investigate the causes of the regional and global differences.

Figure 6 shows that the largest local changes are in general over regions which have experienced large local orographic change (e.g. associated with changes in the Western Cordillera range in North America), especially where this is also associated with lateral shifts of the mountains, which is expressed as regions of localised warming adjacent to localised cooling, for example in the Aptian–Albian (Fig. 6n). However, these local changes are not significant in terms of the global mean. Figure 7 shows how much of the global mean temperature change from Stage-to-Stage is due to changes over land, ocean, or regions which switch between land and ocean. It is clear that for the largest Stage-to-Stage transitions (for example Berriasian–Valanginian, ~ 143–138 Ma; Campanian–Maastrichtian, ~ 77–68 Ma), the ocean is the dominant contributor to the global mean temperature. On average over all the Stage–Stage transitions, the ocean contributes 0.22 °C, the land 0.10 °C, and transitions from land to ocean contribute 0.05 °C. In addition, the temperature change over land correlates very well with the temperature change over ocean (correlation coefficient = 0.74, see Fig. 8a). However, it is unclear whether the ultimate cause of the changes relates to ocean processes (in response e.g. to bathymetry or gateway changes), or whether the ocean is amplifying changes that originate over land.

To investigate this further, we explore the relationship between possible drivers of climate change, and the response. Figure 8b shows the modelled global surface temperature as a function of the change in continental land area. There is a weak negative

Palaeogeographic controls on the climate system

D. J. Lunt et al.

Title Page	
Abstract	Introduction
Conclusions	References
Tables	Figures
◀	▶
◀	▶
Back	Close
Full Screen / Esc	
Printer-friendly Version	
Interactive Discussion	



Palaeogeographic controls on the climate system

D. J. Lunt et al.

Title Page

Abstract

Introduction

Conclusions

References

Tables

Figures



Back

Close

Full Screen / Esc

Printer-friendly Version

Interactive Discussion



correlation (correlation coefficient of -0.47), implying an influence on global temperature from the relative albedo of land compared with ocean. Figure 8c shows the modelled land surface temperature as a function of the change in mean orography. There is a weak positive correlation (correlation coefficient of $+0.49$), implying an influence on land temperature from the local lapse-rate effect. The relationship between global temperature and orography is weaker (not shown, correlation coefficient of $+0.37$), implying that the lapse-rate effect primarily affects local continental temperatures.

We also carry out an energy balance analysis of the causes of temperature change between each Stage, following Heinemann (2009) and Lunt et al. (2012). This allows the global and zonal mean surface temperature change between Stages to be partitioned into contributions from changes in planetary albedo, emissivity, solar constant, and heat transport. We do not save clear-sky flux output from the model, so further partitioning into cloud albedo vs. surface albedo and cloud emissivity vs. greenhouse gas emissivity is not possible in this case. The global mean temperature change correlates well with the contribution due to emissivity (Fig. 8d), but not with the contribution to albedo (Fig. 8e), implying that on a global scale, emissivity feedbacks (due to water vapour and clouds interacting with long wave radiation) play a more consistent role than albedo changes in amplifying the underlying forcing related to the palaeogeographic changes.

It is instructive to focus on the largest transitions in the modelled record. From Fig. 7, we identify 3 such transitions, which all have a global mean temperature change of over 0.7°C (for comparison with the fourth largest transition which is 0.57°C): the Berriasian–Valanginian (~ 142 – 138 Ma), the Aptian–Aptian (~ 119 – 106 Ma), and the Campanian–Maastrichtian (~ 77 – 68 Ma).

3.3.1 Berriasian–Valanginian (Fig. 6r)

This transition is a cooling of 0.84°C in the global mean. In the highest Arctic, there is a warming of more than 10°C , due to a transition from a polar Arctic continent in the Berriasian, to open ocean in the Valanginian. The opposite effect occurs around

the margins of Antarctica around 130–30° W, where there is cooling associated with a transition from open ocean to land. Almost all of the continental changes can be linked directly to orographic changes, via the lapse-rate effect (see Fig. S7 in the Supplement). An exception is in the subtropical ocean just south of North America. Here, there is a cooling whereas from the change in topography a warming is expected (see Fig. S7r in the Supplement).

There is a substantial cooling in the proto-Arctic Ocean. This can be linked to the formation of an island chain at the west end of the Arctic Ocean, which constricts the transport of relatively warm ocean waters into the Arctic, and therefore cools this region. The cooling is amplified by an expansion of Arctic seaice in the Valanginian (Fig. S8 in the Supplement). This cooling effect appears to extend beyond the Arctic, and into the North Pacific. This is also related to a decrease in ocean overturning (see Fig. S10 in the Supplement) and in the extent and magnitude of regions of deep water formation (see Fig. S9 in the Supplement). As such, we attribute this global cooling transition primarily to the closure of the Pacific–Arctic gateway. The timeseries of SST change indicates that the Arctic itself becomes cooler almost immediately (in the first year of the simulation) in the Valanginian. This cool anomaly then spreads southwards, increasing in magnitude over several hundred years, and is amplified at Phase 4 when the barotropic circulation is initialised.

The energy balance analysis for the Berriasian–Valanginian transition (Fig. S12r in the Supplement) shows that, on a global scale, changes in emissivity contribute about 60 % of the cooling, and albedo changes 40 %. As CO₂ is constant across the transition, the emissivity change is a longwave water vapour and cloud feedback effect. The Northern Hemisphere cooling between 50 and 70° N is due to a combination of emissivity and heat transport changes, whereas between 60 and 80° N, at the latitudes of the Arctic Ocean, albedo and emissivity changes dominate.

Palaeogeographic controls on the climate system

D. J. Lunt et al.

Title Page

Abstract

Introduction

Conclusions

References

Tables

Figures



Back

Close

Full Screen / Esc

Printer-friendly Version

Interactive Discussion



3.3.2 Aptian–Albian (Fig. 6n)

This transition is a warming of 0.77°C in the global mean. As for the previous transition, the continental changes are dominated by a lapse-rate effect, and correlate very closely with orographic change (Fig. S7 in the Supplement). Note that some of the largest signals, for example in eastern North America, are essentially artefacts associated with the movement of plates, which manifest as apparent warm–cold dipoles as a mountain range shifts horizontally in the model reference frame, as opposed to true tectonic effects such as uplift. An exception to the strong correlation is in the region of the Andes in South America, where there is a warming, whereas the change in topography would be expected to generate a cooling.

In the ocean, the warmest anomalies are in the northern Pacific, and in the equatorial region that lies between S.America/N.America and Africa/Europe. There is also warming over much of the tropical and subtropical Pacific. However, in the southern Pacific there is a cooling. This is associated with a significant change in ocean circulation. In the Aptian stage, there is a region of deep-water formation off the coast of Antarctica (Fig. S9o in the Supplement), which is associated with a deep overturning cell in the Pacific sector (Fig. S10o in the Supplement). This is much weaker or nonexistent in the Albian stage. This reduction in southern deep water formation reduces surface poleward warm water transport, leading to a reduction in south Pacific temperatures in the Albian compared with the Aptian. The opposite signal in the north Pacific is likely a bipolar seesaw type response, amplified by seaice feedbacks (Fig. S8n and o in the Supplement).

Again, this is supported by the energy balance analysis (Fig. S12n in the Supplement), which shows a cooling contribution due to heat transport changes through most of the region 40 to 80°S , and a warming contribution 50 to 75°N . On a global scale, 10% of the warming is due to the solar constant increase directly (the Albian and Aptian are relatively far apart in time compared to many other consecutive Stages), with emissivity and albedo feedback contributing roughly equally.

Title Page

Abstract

Introduction

Conclusions

References

Tables

Figures



Back

Close

Full Screen / Esc

Printer-friendly Version

Interactive Discussion



3.3.3 Campanian–Maastrichtian (Fig. 6h)

This transition is a warming of 0.74 °C in the global mean. In the ocean, there is warming globally, with the exceptions of the NE Pacific and the southern Atlantic. The largest ocean warmings are in the Pacific sector of the Southern Ocean (associated with a transition from land to ocean) and in the Indian sector of the Southern Ocean. The continental temperatures largely follow topographic change (Fig. S7h in the Supplement), although there is significant warming in northern Africa and western Eurasia which does not appear to be associated with topography.

This Indian sector warming appears to be associated with an increase in deep water formation off the Antarctic coast in this sector (Fig. S9h and i in the Supplement), likely leading to an increase in poleward heat transport from equatorial regions. Although there is some change in the overturning associated with this, it is relatively muted on the global scale (Fig. S10h and i in the Supplement). The reason for the change in ocean circulation is not clear, but it may be due to the northward migration of India, allowing greater transport towards Antarctica in the Maastrichtian stage.

The important role of ocean circulation changes in the Southern Hemisphere is highlighted in the energy balance analysis (Fig. S12 in the Supplement), which shows a significant contribution to the warming polewards of 50° S due to heat transport change. Globally, albedo changes contribute 60 % of the signal, emissivity changes 30 % and solar constant change less than 10 %.

3.3.4 Summary of mechanisms

It appears that the three largest climate transitions are associated with changes in ocean circulation, and driven by quite subtle changes in palaeogeography. Whether climate is ultimately driving ocean circulation, or vice versa, remains difficult to assess without further sensitivity studies. However, ocean circulation changes do seem to be key (for example, the fourth largest transition (Selandian–Thanetian), is also associated with a change in mixed-layer depth (Fig. S9e and f in the Supplement), and overturning

Palaeogeographic controls on the climate system

D. J. Lunt et al.

Title Page

Abstract

Introduction

Conclusions

References

Tables

Figures



Back

Close

Full Screen / Esc

Printer-friendly Version

Interactive Discussion



Palaeogeographic controls on the climate system

D. J. Lunt et al.

Title Page

Abstract

Introduction

Conclusions

References

Tables

Figures



Back

Close

Full Screen / Esc

Printer-friendly Version

Interactive Discussion



into account the effects of rotating plates. Getech Plc have provided us with palaeo-longitudes and palaeolatitudes for each model gridcell and each Stage, which allows us to ascertain the palaeolocation of any modern location, consistent with the palaeogeographies used in the climate model simulations. The palaeolocations of seven key sites (Blake Nose, Demerara Rise, Falkland Plateau, Walvis Ridge, Maud Rise, Tanzania, and the Saxony Basin), which have previously been used to reconstruct CPE SSTs from planktic $\delta^{18}\text{O}$, is shown in Fig. 9a. This shows that all the sites move a significant distance over the course of the CPE. Note that the “oldest” location is different for each site, as some sites exist on ocean crust which was not formed until after the earliest Cretaceous (e.g. Walvis Ridge).

Figure 9b shows the modelled annual mean surface air temperature at each of these seven locations, as climate changes through the CPE and as the plates underlying each site move. These variations are large; the maximum temperature in the CPE minus minimum temperature in the CPE varies from 5.6°C at Demerara Rise, to 12.3°C at Maud Rise. This is in the context of a global mean modelled climate which is only varying by a fraction of a degree over this interval (Fig. 5). These modelled temperature records are the “adjustment factor” we describe above.

Some of the temporal variations in the adjustment factor, in particular at Saxony Basin, Tanzania, and Falkland Plateau, are due to transitions from the site being oceanic to continental (Fig. 9b; filled circles compared with open triangles). For coastal sites, such as Tanzania, the transitions may be an artefact of the coarse resolution of the model palaeolatitudes and longitudes, which are $3.75^\circ \times 2.5^\circ$, and which cannot therefore distinguish correctly between land and ocean near the coast. Some sites are characterised by relatively stable modelled temperatures (and therefore small adjustment factors) over 10’s of millions of years, for example Demerara Rise and Blake Nose during the late Cretaceous.

It is not possible with our current experimental design to partition the component of the adjustment factor due to solar constant from that due to palaeogeography; however, it is possible to partition the effect due to plate movements. Figure S11 in the

Palaeogeographic controls on the climate system

D. J. Lunt et al.

Title Page

Abstract

Introduction

Conclusions

References

Tables

Figures



Back

Close

Full Screen / Esc

Printer-friendly Version

Interactive Discussion



5 nental and marine settings). This can be interpreted as a map indicating places where future proxies could be targeted in order to reconstruct the purest CO₂-induced temperature change, where the complicating contributions of other (palaeogeographical, solar, and plate movement) processes are minimised (low values in Fig. 11 represent the “best” regions in this context). White regions indicate that the modern crust was not present at the beginning of the CPE. Figures 11b–d are similar, but show the total change in temperature across the Eocene (d), the Eocene–Palaeocene (c), and the Eocene–Palaeocene-early Cretaceous (b). Not all of the “best” regions will have suitable sedimentary material, obviously, but, combined with all other considerations, this work could provide useful information for supporting targets for drilling localities and outcrop studies.

4 Discussion

15 It is anticipated that the results from these simulations will be of interest to the palaeoclimate data community; as such, we make the results available on our website: <http://www.bridge.bris.ac.uk/resources/simulations>, including variables not discussed in this paper. In addition, in the Supplement we provide the raw data which underlies Figs. 9 and 11, in netcdf and ascii format, which will allow others to develop their own adjustments, over any period in the CPE, for any site in the world.

20 The Eocene simulations (Ypresian, Lutetian, Bartonian, and Priabonian) described in this paper have been discussed in a previous publication (Inglis et al., 2015), as has a lower CO₂ simulation of the Priabonian simulation (Kennedy et al., 2015), and a less spun-up version of the Maastrichtian simulation (Brown, 2013). In addition, in future studies we expect to investigate many aspects of the simulations which have not been possible in the scope of this study, including the evolution of monsoon systems, ENSO, 25 vegetation, and atmospheric circulation. Furthermore, we intend to carry out sensitivity studies, especially to CO₂ in order to investigate the evolution of climate sensitivity through geological time.

Palaeogeographic controls on the climate system

D. J. Lunt et al.

Title Page

Abstract

Introduction

Conclusions

References

Tables

Figures



Back

Close

Full Screen / Esc

Printer-friendly Version

Interactive Discussion



However, there are some aspects of the simulations which could be modified and improved, although we do not think that they will have a first-order effect on our results. The following is not a complete list, but includes the main aspects that we intend to improve as we commence Phase 5 of the ensemble.

The version of the model used in this study has received little or no tuning. The internal model parameters in the atmosphere are identical to those in HadCM3 (Gordon et al., 2000), which did receive some (largely undocumented) tuning at the UK Met Office. However, compared with HadCM3, our model has a lower resolution ocean and a different land-surface scheme. In addition, the ozone correction discussed in Sect. 2.5 cools the climate somewhat. Furthermore, the subgridscale parameters derived from the Getech $0.5^\circ \times 0.5^\circ$ resolution palaeogeographies are not necessarily consistent with those derived from higher resolution observational datasets. As such, the modern climate for this version of the model has greater biases than the HadCM3 model from which it is derived. Future work will involve tuning the model, using techniques such as those developed by Irvine et al. (2013).

In order to maintain stability in the atmosphere and ocean, some Stages received more or less smoothing of topography or bathymetry than others (see Table 1). In Phase 5, we will be more consistent, and apply the same amount of smoothing to all Stages.

There are still trends in the ocean temperatures, at all depths (see Fig. 4). Although computational constraints mean that no GCM of this complexity could currently be run to full equilibrium, and we argue that the main findings presented here will not be affected significantly by further spinup, we do aim to run Phase 5 for a further 1000 years in order to further approach equilibrium.

Getech Plc provide maps of runoff basins and nodes, but these are not currently used. Instead, as discussed in Sect. 2.5, water is routed downhill according to the model resolution topography. In Phase 5 we will make use of the observational constraints on river basins and river mouths by using the Getech maps.

Palaeogeographic controls on the climate system

D. J. Lunt et al.

Title Page

Abstract

Introduction

Conclusions

References

Tables

Figures



Back

Close

Full Screen / Esc

Printer-friendly Version

Interactive Discussion



We have not been consistent in our definition of islands for the purposes of the barotropic circulation calculation. For example, in some Stages single gridcell islands are defined as such, and in others they are not (see Fig. S4 in the Supplement). Furthermore, we have not defined the continent of Antarctica and Australasia as an island in the mid Cretaceous simulations, which could affect the flow through the Tethys–Pacific seaway and Drake Passage (see discussion in Kennedy et al., 2015).

The model does not rigorously conserve water, due to the build-up of snow on polar continents, the loss of water in endorheic regions, and a salinity cap which affects inland basins. In the modern, a prescribed freshwater flux is applied in polar regions, in an attempt to mitigate against salinity drift in long simulations. However, in these simulations we do not apply such a correction. In Phase 5 we will diagnose a freshwater flux in order to maintain constant ocean mean salinity.

5 Conclusions

1. We have carried out a set of 19 GCM simulations covering 115 million years, one for each Stage, from the earliest Cretaceous to the latest Eocene, with constant CO_2 but varying palaeogeography and solar constant (Table 1). All simulations are within 1 W m^{-2} of equilibrium after more than 1400 years of simulation.
2. The global mean temperatures across the simulations are remarkably constant, with a trend of only $0.004 \text{ }^\circ\text{C million years}^{-1}$ (Fig. 5). The lack of trend results from a cancelling of effects due to changing solar constant with effects due to changing palaeogeography.
3. There is also little scatter around the trend, $\sim \pm 0.5 \text{ }^\circ\text{C}$ (Fig. 7). The scatter correlates weakly with changing land area, indicating the albedo contrast between land and ocean plays a role; continental temperatures correlate weakly with mean orography, indicating lapse rate and area above snowline also plays a role (Fig. 8). Energy balance analysis indicates that the solar and palaeogeographic forcing is

Palaeogeographic controls on the climate system

D. J. Lunt et al.

Title Page	
Abstract	Introduction
Conclusions	References
Tables	Figures
◀	▶
◀	▶
Back	Close
Full Screen / Esc	
Printer-friendly Version	
Interactive Discussion	



amplified by albedo and emissivity feedbacks, with emissivity changes (due to water vapour and clouds interacting with longwave radiation) being the most consistent feedback.

4. The largest Stage–Stage transitions through the CPE are associated with changes in the mode of ocean circulation. For example, the largest transition, Berriasian–Valanginian, is associated with a reduction in deepwater formation in the North Pacific, and a reduction in the meridional positively overturning cell; the second largest transition, Aptian–Albian, is associated with a reduction in deepwater formation off the coast of Antarctica, and a reduction in the negatively overturning cell. In some cases, these ocean circulation changes can be directly related to palaeogeographic change associated with gateway opening or closing, for example the isolation of the Arctic at the Berriasian–Valanginian transition.
5. Although the global mean changes are relatively small across the CPE, local temperature changes are much larger (Fig. 11). This has implications for interpretations of proxy records. In particular, our results allow the non-CO₂ (i.e. palaeogeographic and solar constant) components of proxy records to be removed, through the application of an adjustment factor, leaving a global component associated with carbon cycle change. This adjustment factor is illustrated for 7 key sites in the CPE (Fig. 9), and applied to proxy data from Falkland plateau, and data provided so that similar adjustments can be made to any site and for any time period within the CPE.

The Supplement related to this article is available online at doi:10.5194/cpd-11-5683-2015-supplement.

Acknowledgements. Work carried out in the framework of NERC grants Descent into the Icehouse (NE/I005714/1), Paleopolar (NE/I005722/1,NE/I005501/2), and CPE

(NE/K014757/1,NE/K012479/1) all contributed to this paper. We thank Getech Plc for providing the palaeogeographies and plate rotations. This work was carried out using the computational facilities of the Advanced Computing Research Centre, University of Bristol – <http://www.bris.ac.uk/acrc/>.

References

- Barron, E. J. and Peterson, W. H.: Mid-Cretaceous ocean circulation: results from model sensitivity studies, *Paleoceanography*, 5, 319–337, 1990. 5687
- Barron, E. J. and Washington, W. M.: The role of geographic variables in explaining paleoclimates: results from Cretaceous Climate Model sensitivity studies, *J. Geophys. Res.*, 89, 1267–1279, 1984. 5685, 5687
- Barron, E. J., Sloan II, J. L., and Harrison, C. G. A.: Potential significance of land-sea distribution and surface albedo variations as a climatic forcing factor; 180 M.Y. to the present, *Palaeogeogr. Palaeoclimatol.*, 30, 17–40, 1980. 5686, 5687
- Barron, E. J., Fawcett, P. J., Peterson, W. H., Pollard, D., and Thompson, S. L.: A ‘simulation’ of mid-Cretaceous climate, *Paleoceanography*, 10, 953–962, 1995. 5685, 5687
- Beerling, D. and Royer, D.: Convergent Cenozoic CO₂ history, *Nat. Geosci.*, 4, 418–420, 2011. 5690, 5694
- Beerling, D. J., Fox, A., Stevenson, D. S., and Valdes, P. J.: Enhanced chemistry-climate feedbacks in past greenhouse worlds, *P. Natl. Acad. Sci. USA*, 108, 9770–9775, 2011. 5690
- Bice, K. L. and Marotzke, J.: Could changing ocean circulation have destabilized methane hydrate at the Paleocene/Eocene boundary?, *Paleoceanography*, 17, 1018, doi:10.1029/2001PA000678, 2002. 5688
- Bice, K. L., Huber, B. T., and Norris, R. D.: Extreme polar warmth during the Cretaceous greenhouse? Paradox of the late Turonian $\delta^{18}\text{O}$ record at Deep Sea Drilling Project Site 511, *Paleoceanography*, 18, 1031, doi:10.1029/2002PA000848, 2003. 5688, 5701
- Bice, K. L., Birgel, D., Meyers, P. A., Dahl, K. A., Hinrichs, K.-U., and Norris, R. D.: A multiple proxy and model study of Cretaceous upper ocean temperatures and atmospheric CO₂ concentrations, *Paleoceanography*, 21, PA2002, doi:10.1029/2005PA001203, 2006. 5688

Palaeogeographic controls on the climate system

D. J. Lunt et al.

Title Page

Abstract

Introduction

Conclusions

References

Tables

Figures



Back

Close

Full Screen / Esc

Printer-friendly Version

Interactive Discussion



Palaeogeographic controls on the climate system

D. J. Lunt et al.

[Title Page](#)[Abstract](#)[Introduction](#)[Conclusions](#)[References](#)[Tables](#)[Figures](#)[Back](#)[Close](#)[Full Screen / Esc](#)[Printer-friendly Version](#)[Interactive Discussion](#)

Bornemann, A., Norris, R., Friedrich, O., Beckmann, B., Schouten, S., Sinninghe-Damsté, J., Vogel, J., Hofmann, P., and Wagner, T.: Isotopic evidence for glaciation during the Cretaceous supergreenhouse, *Science*, 319, 189–192, 2008. 5701

Bradshaw, C. D., Lunt, D. J., Flecker, R., Salzmann, U., Pound, M. J., Haywood, A. M., and Eronen, J. T.: The relative roles of CO₂ and palaeogeography in determining late Miocene climate: results from a terrestrial model–data comparison, *Clim. Past*, 8, 1257–1285, doi:10.5194/cp-8-1257-2012, 2012. 5691

Brown, R.: The climate of Middle Earth, *J. Hobbitlore*, 1, 1–8, 2013. 5704

Caballero, R. and Huber, M.: State-dependent climate sensitivity in past warm climates and its implications for future climate projections, *P. Natl. Acad. Sci. USA*, 110, 14162–14167, 2013. 5687

Caldeira, K. and Kasting, J. F.: The life span of the biosphere revisited, *Nature*, 360, 721–723, 1992. 5691, 5716

Cox, P., Betts, R., Bunton, C., Essery, R., Rowntree, P. R., and Smith, J.: The impact of new land-surface physics on the GCM simulation and climate sensitivity, *Clim. Dynam.*, 15, 183–203, 1999. 5691

Cox, P. M., Betts, R. A., Jones, C. D., Spall, S. A., and Totterdell, I. J.: Modelling vegetation and the carbon cycle as interactive elements of the climate system, in: *Meteorology at the Millennium*, edited by: Pearce, R., Academic Press, San Diego CA, USA, 259–279, 2001. 5691

Cramer, B. S., Toggweiler, J. R., Wright, J. D., Katz, M. E., and Miller, K. G.: Ocean overturning since the Late Cretaceous: inferences from a new benthic foraminiferal isotope compilation, *Paleoceanography*, 24, PA4216, doi:10.1029/2008PA001683, 2009. 5685, 5693, 5715, 5719

Donnadieu, Y., Pierrehumbert, R., Jacob, R., and Fluteau, F.: Modelling the primary control of paleogeography on Cretaceous climate, *Earth Planet. Sc. Lett.*, 248, 426–437, 2006. 5687, 5688

Donnadieu, Y., Godd ris, Y., and Bouttes, N.: Exploring the climatic impact of the continental vegetation on the Mesozoic atmospheric CO₂ and climate history, *Clim. Past*, 5, 85–96, doi:10.5194/cp-5-85-2009, 2009. 5691

Erbacher, J., Friedrich, O., Wilson, P., Lehmann, J., and Weiss, W.: Short-term warming events during the boreal Albian (mid-Cretaceous), *Geology*, 39, 223–226, 2011. 5701

Palaeogeographic controls on the climate system

D. J. Lunt et al.

Title Page

Abstract

Introduction

Conclusions

References

Tables

Figures



Back

Close

Full Screen / Esc

Printer-friendly Version

Interactive Discussion



- Forster, A., Schouten, S., Baas, M., and Sinninghe Damste, J. S.: Mid-Cretaceous (Albian–Santonian) sea surface temperature record of the tropical Atlantic Ocean, *Geology*, 35, 919–922, 2007. 5701
- Foster, G. L., Lunt, D. J., and Parrish, R. R.: Mountain uplift and the glaciation of North America – a sensitivity study, *Clim. Past*, 6, 707–717, doi:10.5194/cp-6-707-2010, 2010. 5686
- Franks, P. J., Royer, D. L., Beerling, D. J., de Water, P. K. V., Cantrill, D. J., Barbour, M. M., and Berry, J. A.: New constraints on atmospheric CO₂ concentration for the Phanerozoic, *Geophys. Res. Lett.*, 41, 4685–4694, doi:10.1002/2014GL060457, 2014. 5687
- Friedrich, O., Erbacher, J., Moriya, K., Wilson, P., and Kuhnert, H.: Warm saline intermediate waters in the Cretaceous tropical Atlantic Ocean, *Nat. Geosci.*, 1, 453–457, 2008. 5701
- Friedrich, O., Norris, R. D., and Erbacher, J.: Evolution of middle to Late Cretaceous oceans – a 55 m.y. record of Earth’s temperature and carbon cycle, *Geology*, 40, 107–110, 2012. 5685, 5715
- Gordon, C., Cooper, C., Senior, C. A., Banks, H., Gregory, J. M., Johns, T. C., Mitchell, J. F. B., and Wood, R. A.: The simulation of SST, sea ice extents and ocean heat transports in a version of the Hadley Centre coupled model without flux adjustments, *Clim. Dynam.*, 16, 147–168, 2000. 5691, 5705
- Gough, D.: Solar interior structure and luminosity variations, *Sol. Phys.*, 74, 21–34, 1981. 5686, 5691, 5714, 5716
- Hansen, J., Sato, M., Russell, G., and Kharecha, P.: Climate sensitivity, sea level and atmospheric carbon dioxide, *Philos. T. R. Soc. A*, 371, 20120294, doi:10.1098/rsta.2012.0294, 2013. 5685, 5693, 5694, 5715, 5719
- Heinemann, M.: Warm and sensitive Paleocene–Eocene climate, *Reports on Earth System Science*, 70, Max Planck Institute for Meteorology, Hamburg, Germany, 2009. 5697
- Honisch, B., Ridgwell, A., Schmidt, D. N., Thomas, E., Gibbs, S. J., Sluijs, A., Zeebe, R., Kump, L., Martindale, R. C., Greene, S. E., Kiessling, W., Ries, J., Zachos, J. C., Royer, D. L., Barker, S., Marchitto, T. M., Moyer, R., Pelejero, C., Ziveri, P., Foster, G. L., and Williams, B.: The geological record of ocean acidification, *Science*, 335, 1058–1063, 2012. 5687, 5690, 5717
- Huber, B. T., Hodell, D. A., and Hamilton, C. P.: Middle-Late Cretaceous climate of the southern high latitudes: stable isotopic evidence for minimal equator-to-pole thermal gradients, *Geol. Soc. Am. Bull.*, 107, 1164–1191, 1995. 5701

Palaeogeographic controls on the climate system

D. J. Lunt et al.

Title Page

Abstract

Introduction

Conclusions

References

Tables

Figures



Back

Close

Full Screen / Esc

Printer-friendly Version

Interactive Discussion



- Huber, B. T., Norris, R. D., and MacLeod, K. G.: Deep-sea paleotemperature record of extreme warmth during the Cretaceous, *Geology*, 30, 123–126, 2002. 5701
- Huber, M. and Caballero, R.: The early Eocene equable climate problem revisited, *Clim. Past*, 7, 603–633, doi:10.5194/cp-7-603-2011, 2011. 5688
- 5 Inglis, G. N., Farnsworth, A., Lunt, D., Foster, G., Hollis, C., Pagani, M., Jardine, P., Pearson, P., Markwick, P., Raynman, L., Galsworthy, A., and Pancost, R.: Descent towards the icehouse: Eocene sea surface cooling inferred from GDGT distributions, *Paleoceanography*, 30, 1000–1020, doi:10.1002/2014PA002723, 2015. 5704
- Irvine, P. J., Gregoire, L. J., Lunt, D. J., and Valdes, P. J.: An efficient method to generate a perturbed parameter ensemble of a fully coupled AOGCM without flux-adjustment, *Geosci. Model Dev.*, 6, 1447–1462, doi:10.5194/gmd-6-1447-2013, 2013. 5705
- 10 Jenkyns, H. C., Schouten-Huibers, L., Schouten, S., and Sinninghe Damsté, J. S.: Warm Middle Jurassic–Early Cretaceous high-latitude sea-surface temperatures from the Southern Ocean, *Clim. Past*, 8, 215–226, doi:10.5194/cp-8-215-2012, 2012. 5701
- 15 Kennedy, A., Farnsworth, A., Lunt, D., and Lear, C.: Palaeogeographic control on the atmospheric and oceanic impacts of Antarctic glaciation at the Eocene–Oligocene boundary, *Philos. T. R. Soc. A*, 373, 20140419, doi:10.1098/rsta.2014.0419, 2015. 5704, 5706
- Lauderdale, J. M., Naveira Garabato, A. C., Oliver, K. I., Follows, M. J., and Williams, R. G.: Wind-driven changes in Southern Ocean residual circulation, ocean carbon reservoirs and atmospheric CO₂, *Clim. Dynam.*, 41, 2145–2164, 2013. 5686
- 20 Linnert, C., Robinson, S., Lees, J., Bown, P., Perez-Rodriguez, I., Petrizzo, M., Falzoni, F., Littler, K., Arz, J., and Russell, E.: Evidence for global cooling in the Late Cretaceous, *Nature Communications*, 5, 4194, doi:10.1038/ncomms5194, 2014. 5701
- Littler, K., Robinson, S., Bown, P., Nederbragt, A., and Pancost, R.: High sea-surface temperatures during the Early Cretaceous Epoch, *Nat. Geosci.*, 4, 169–172, 2011. 5701
- 25 Loftson, C. A., Lunt, D. J., and Francis, J. E.: Investigating vegetation–climate feedbacks during the early Eocene, *Clim. Past*, 10, 419–436, doi:10.5194/cp-10-419-2014, 2014. 5691, 5695
- Lunt, D. J., Valdes, P. J., Dunkley Jones, T., Ridgwell, A., Haywood, A. M., Schmidt, D. N., Marsh, R., and Maslin, M.: CO₂-driven ocean circulation changes as an amplifier of Paleocene–Eocene thermal maximum hydrate destabilization, *Geology*, 38, 875–878, 2010. 5691
- 30 Lunt, D. J., Dunkley Jones, T., Heinemann, M., Huber, M., LeGrande, A., Winguth, A., Loftson, C., Marotzke, J., Roberts, C. D., Tindall, J., Valdes, P., and Winguth, C.: A model–data

Palaeogeographic controls on the climate system

D. J. Lunt et al.

[Title Page](#)

[Abstract](#)

[Introduction](#)

[Conclusions](#)

[References](#)

[Tables](#)

[Figures](#)



[Back](#)

[Close](#)

[Full Screen / Esc](#)

[Printer-friendly Version](#)

[Interactive Discussion](#)



- comparison for a multi-model ensemble of early Eocene atmosphere–ocean simulations: EoMIP, *Clim. Past*, 8, 1717–1736, doi:10.5194/cp-8-1717-2012, 2012. 5688, 5697
- Luyendyk, B. P., Forsyth, D., and Phillips, J. D.: Experimental approach to the paleocirculation of the oceanic surface waters, *Geol. Soc. Am. Bull.*, 83, 2649–2664, 1972. 5687
- 5 MacLeod, K., Huber, B., Berrocoso, A., and Wendler, I.: A stable and hot Turonian without glacial $\delta^{18}\text{O}$ excursions is indicated by exquisitely preserved Tanzanian *Foraminifera*, *Geology*, 41, 1083–1086, 2013. 5701
- Markwick, P. J. and Valdes, P. J.: Palaeo-digital elevation models for use as boundary conditions in coupled ocean–atmosphere GCM experiments: a Maastrichtian (late Cretaceous)
- 10 example, *Palaeogeogr. Palaeoclimatol.*, 213, 37–63, 2004. 5689
- Martinez-Boti, M., Foster, G., Chalk, T., Rohling, E., Sexton, P., Lunt, D., Pancost, R., Badger, M., and Schmidt, D.: Plio–Pleistocene climate sensitivity evaluated using high-resolution CO_2 records, *Nature*, 518, 49–54, 2015. 5687
- Pagani, M., Huber, M., Liu, Z., Bohaty, S. M., Henderiks, J., Sijp, W., Krishnan, S., and DeConto, R. M.: The role of carbon dioxide during the onset of Antarctic glaciation, *Science*,
- 15 334, 1261–1264, 2011. 5694
- Pearson, P. N., Foster, G. L., and Wade, B. S.: Atmospheric carbon dioxide through the Eocene–Oligocene climate transition, *Nature*, 461, 1110–1113, 2009. 5694
- Poulsen, C. J., Barron, E. J., Arthur, M. A., and Peterson, W. H.: Response of the mid-Cretaceous global oceanic circulation to tectonic and CO_2 forcings, *Paleoceanography*, 16,
- 20 1–17, 2001. 5687, 5688
- Poulsen, C. J., Gendaszek, A. S., and Jacob, R. L.: Did the rifting of the Atlantic Ocean cause the Cretaceous thermal maximum?, *Geology*, 31, 115–118, 2003. 5687, 5688
- Poulsen, C. J., Pollard, D., and White, T. S.: General circulation model simulation of the $\delta^{18}\text{O}$ content of continental precipitation in the middle Cretaceous: a model–proxy comparison,
- 25 *Geology*, 35, 199–202, 2007. 5688
- Raymo, M. E., Ruddiman, W. F., and Froelich, P. N.: Influence of late Cenozoic mountain building on ocean geochemical cycles, *Geology*, 16, 649–653, 1988. 5686
- Royer, D., Pagani, M., and Beerling, D. J.: Geobiological constraints on Earth system sensitivity to CO_2 during the Cretaceous and Cenozoic, *Geobiology*, 10, 298–310, 2012. 5690
- 30 Ruddiman, W. F. and Kutzbach, J. E.: Forcing of Late Cenozoic Northern Hemisphere climate by plateau uplift in southern Asia and the American West, *J. Geophys. Res.-Atmos.*, 94, 18409–18427, 1989. 5686

Palaeogeographic controls on the climate system

D. J. Lunt et al.

Title Page

Abstract

Introduction

Conclusions

References

Tables

Figures



Back

Close

Full Screen / Esc

Printer-friendly Version

Interactive Discussion



- Scotese, C.: Atlas of Earth History, University of Texas, Arlington, 2001. 5686
- Sellwood, B. W., Price, G. D., and Valdes, P. J.: Cooler estimates of Cretaceous temperatures, *Nature*, 370, 453–455, 1994. 5687
- Spicer, R. A., Ahlberg, A., Herman, A. B., Hofmann, C.-C., Raikevich, M., Valdes, P. J., and Markwick, P. J.: The Late Cretaceous continental interior of Siberia: a challenge for climate models, *Earth Planet. Sc. Lett.*, 267, 228–235, 2008. 5688
- Winguth, A., Shellito, C., Shields, C., and Winguth, C.: Climate response at the Paleocene–Eocene thermal maximum to greenhouse gas forcing – a model study with CCSM3, *J. Climate*, 23, 2562–2584, 2010. 5688
- Zhang, Y., Pagani, M., Liu, Z., Bohaty, S. M., and DeConto, R.: A 40-million-year history of atmospheric CO₂, *Philos. T. R. Soc. A*, 371, 20130096, doi:10.1098/rsta.2013.0096, 2013. 5687
- Zhang, Z., Nisancioglu, K. H., Flatøy, F., Bentsen, M., Bethke, I., and Wang, H.: Tropical seaways played a more important role than high latitude seaways in Cenozoic cooling, *Clim. Past*, 7, 801–813, doi:10.5194/cp-7-801-2011, 2011. 5686
- Zhou, J., Poulsen, C. J., Pollard, D., and White, T. S.: Simulation of modern and middle Cretaceous marine $\delta^{18}\text{O}$ with an ocean–atmosphere general circulation model, *Paleoceanography*, 23, PA3223, doi:10.1029/2008PA001596, 2008. 5688
- Zhou, J., Poulsen, C. J., Rosenbloom, N., Shields, C., and Briegleb, B.: Vegetation-climate interactions in the warm mid-Cretaceous, *Clim. Past*, 8, 565–576, doi:10.5194/cp-8-565-2012, 2012. 5687, 5691

Palaeogeographic controls on the climate system

D. J. Lunt et al.

Title Page

Abstract

Introduction

Conclusions

References

Tables

Figures



Back

Close

Full Screen / Esc

Printer-friendly Version

Interactive Discussion



Table 1. Summary of all model simulations. The age column shows the age of the middle of the respective Stage. The solar constants are calculated using these ages according to the formula described in Gough (1981). The smoothing indicates the changes that had to applied to each Stage to ensure stability. F = fourier filtering at high latitudes, Ar = flat Arctic ocean, An = flat polar Southern ocean, O1 = polar orographic smoothing, O2 = polar orographic smoothing and capping of polar topography, L = minor changes to land–sea mask. P3 and P4 indicate Phases 3 and 4 of the simulations.

Stage	Age (Ma)	Solar constant ($W m^{-2}$)	CO ₂ (ppmv)	smoothing P3	smoothing P4
Eocene					
Priabonian	35.7	1360.86	1120		
Bartonian	39.0	1360.48	1120		
Lutetian	44.7	1359.83	1120	F	F
Ypresian	52.6	1358.91	1120	F Ar	Ar
Paleocene					
Thanetian	57.3	1358.37	1120	F	
Selandian	60.6	1357.99	1120	F	Ar
Danian	63.9	1357.61	1120	Ar	Ar
Cretaceous					
Maastrichtian	68.2	1357.18	1120		An
Campanian	77.1	1356.16	1120	F	F O1 Ar L
Santonian	84.7	1355.24	1120	Ar	Ar
Coniacian	87.6	1354.92	1120	F Ar An	F Ar An
Turonian	91.4	1354.49	1120	F An	F Ar
Cenomanian	96.4	1353.90	1120	Ar O1	Ar O1
Albian	105.8	1352.82	1120	Ar L	Ar L
Aptian	118.5	1351.38	1120		Ar
Barremian	127.5	1350.36	1120		
Hauterivian	133.2	1349.72	1120	O1	Ar O1
Valanginian	138.3	1349.13	1120	Ar	Ar
Berriasian	142.9	1348.65	1120	O2	Ar O2

Palaeogeographic controls on the climate system

D. J. Lunt et al.

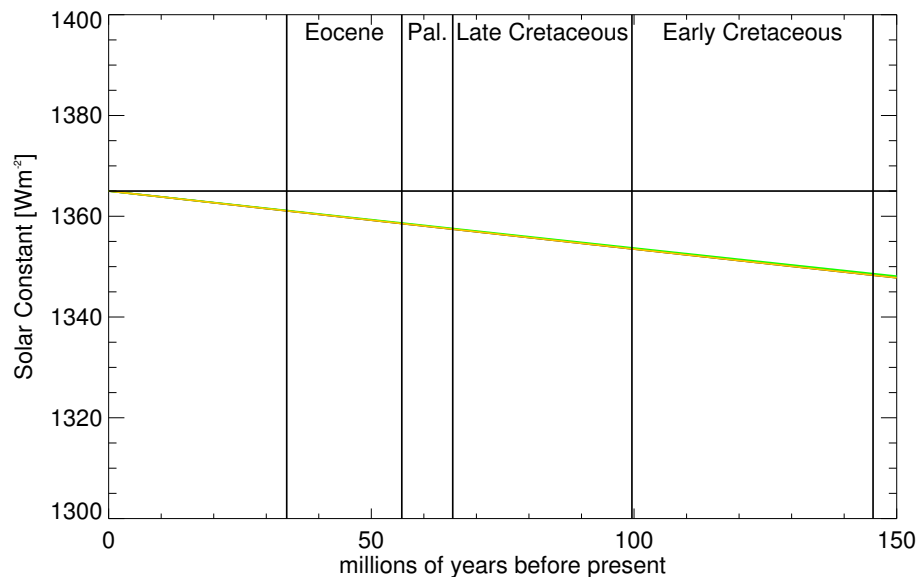


Figure 2. The values of solar constant since the earliest Cretaceous, calculated from Gough (1981) and used for the CPE simulations in this paper (green line), and from Caldeira and Kasting (1992) (orange line).

[Title Page](#)[Abstract](#)[Introduction](#)[Conclusions](#)[References](#)[Tables](#)[Figures](#)[Back](#)[Close](#)[Full Screen / Esc](#)[Printer-friendly Version](#)[Interactive Discussion](#)

Palaeogeographic controls on the climate system

D. J. Lunt et al.

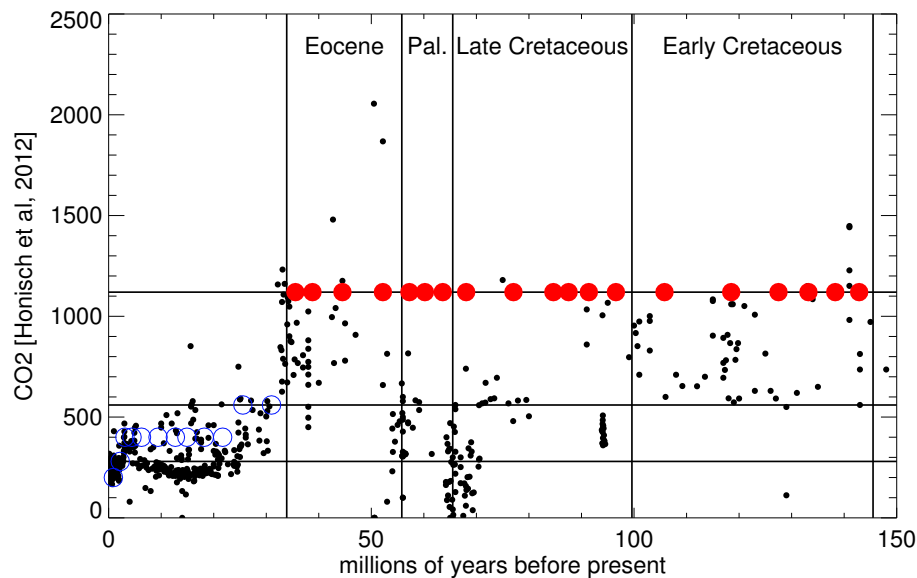


Figure 3. CO₂ as compiled by Honisch et al. (2012) (small dots). Overlain is the CO₂ concentration in each simulation described in this paper (red dots). The open blue circles show CO₂ concentration in a set of model simulations of the Oligocene and Neogene, which are not discussed in this paper but are provided for reference. Horizontal black lines show 280, 560, and 1120 ppmv.

[Title Page](#)[Abstract](#)[Introduction](#)[Conclusions](#)[References](#)[Tables](#)[Figures](#)[Back](#)[Close](#)[Full Screen / Esc](#)[Printer-friendly Version](#)[Interactive Discussion](#)

Palaeogeographic controls on the climate system

D. J. Lunt et al.

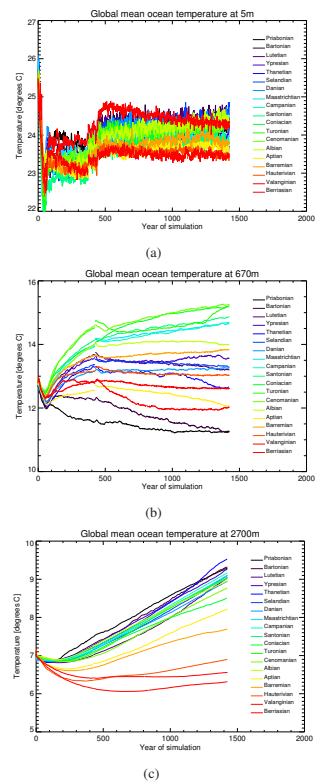


Figure 4. Modelled evolution of global mean ocean temperature [$^{\circ}\text{C}$] in each CPE simulation at three depths: **(a)** surface (5 m), **(b)** 670 m, **(c)** 2.7 km.

[Title Page](#)
[Abstract](#)
[Introduction](#)
[Conclusions](#)
[References](#)
[Tables](#)
[Figures](#)

[Back](#)
[Close](#)
[Full Screen / Esc](#)
[Printer-friendly Version](#)
[Interactive Discussion](#)

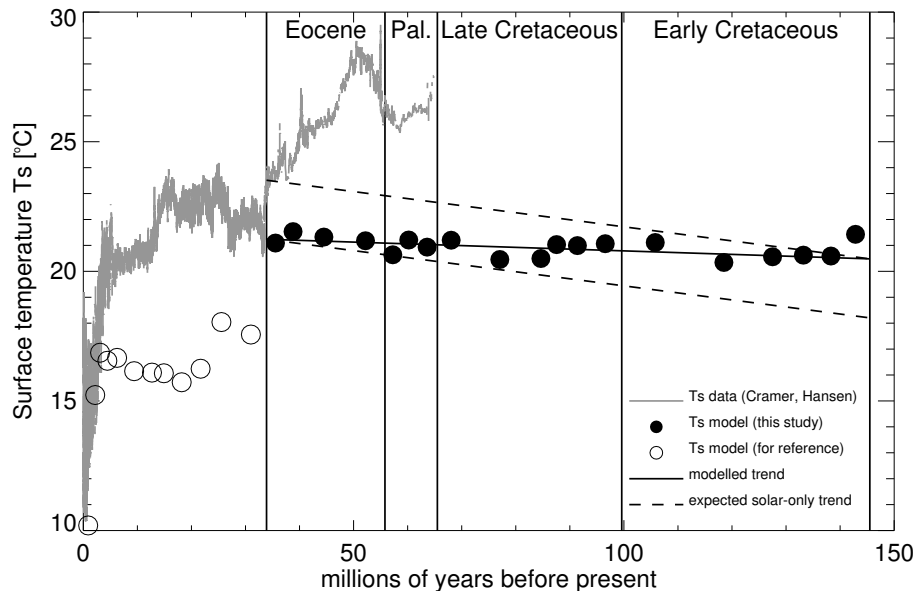



Figure 5. The global MAT for each Stage of the CPE at $4 \times \text{CO}_2$ (black filled circles) plotted over a surface temperature record produced by applying the methodologies of Hansen et al. (2013) to the Cramer et al. (2009) $\delta^{18}\text{O}_{\text{benthic}}$ data, and applying a 10-point running average (grey line). The open circles show model results for the Oligocene and Neogene, with lower CO_2 , which are not discussed in this paper but are provided for reference. The modelled trend (ignoring the outlying Berriasian stage) is shown as a solid line, and the expected trend assuming solar forcing only is shown as a pair of dashed lines which start/end at the beginning/end of the modelled trend.

Palaeogeographic controls on the climate system

D. J. Lunt et al.

[Title Page](#)

[Abstract](#) | [Introduction](#)

[Conclusions](#) | [References](#)

[Tables](#) | [Figures](#)

[◀](#) | [▶](#)

[◀](#) | [▶](#)

[Back](#) | [Close](#)

[Full Screen / Esc](#)

[Printer-friendly Version](#)

[Interactive Discussion](#)



Palaeogeographic controls on the climate system

D. J. Lunt et al.

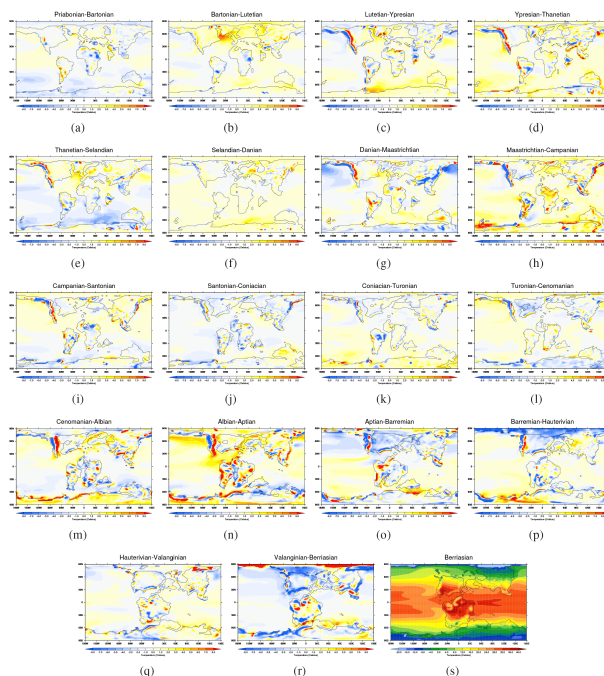


Figure 6. (a–r) Annual mean surface air temperature (at 1.5 m) for each geological Stage, expressed as an anomaly relative to the previous Stage. (a) Priabonian–Bartonian, (b) Bartonian–Lutetian, (c) Lutetian–Ypresian, (d) Ypresian–Thanetian (e) Thanetian–Selandian, (f) Selandian–Danian, (g) Danian–Maastrichtian, (h) Maastrichtian–Campanian, (i) Campanian–Santonian, (j) Santonian–Coniacian, (k) Coniacian–Turonian, (l) Turonian–Cenomanian, (m) Cenomanian–Albian, (n) Albian–Aptian, (o) Aptian–Barremian, (p) Barremian–Hauterivian, (q) Hauterivian–Valanginian, (r) Valanginian–Berriasian. (s) Annual mean surface air temperature (at 1.5 m) for the Berriasian stage.

Palaeogeographic controls on the climate system

D. J. Lunt et al.

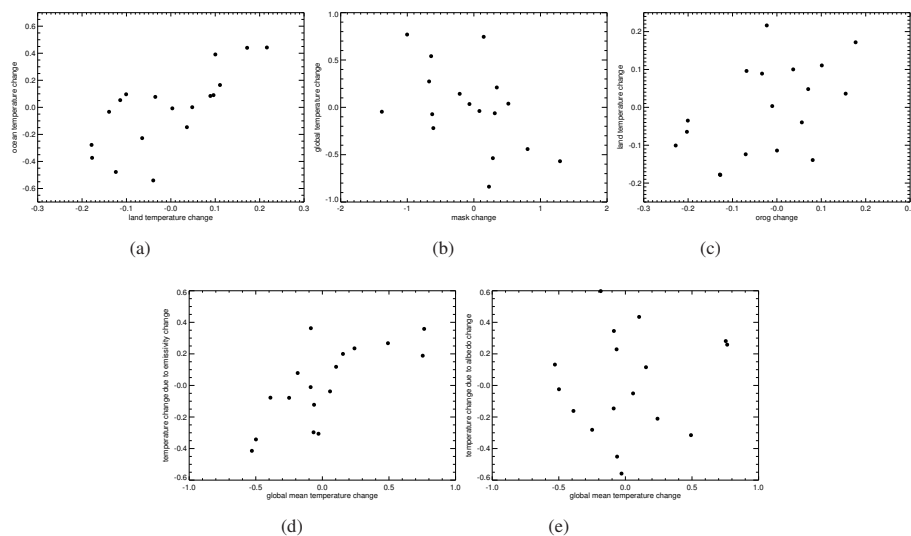


Figure 8. Plots showing the relationship between Stage–Stage changes in **(a)** continental temperature and ocean temperature, **(b)** continental area and global mean temperature, **(c)** orography and continental temperature, **(d)** global mean temperature and emissivity, and **(e)** global mean temperature and albedo.

Title Page

Abstract

Introduction

Conclusions

References

Tables

Figures



Back

Close

Full Screen / Esc

Printer-friendly Version

Interactive Discussion



Palaeogeographic controls on the climate system

D. J. Lunt et al.

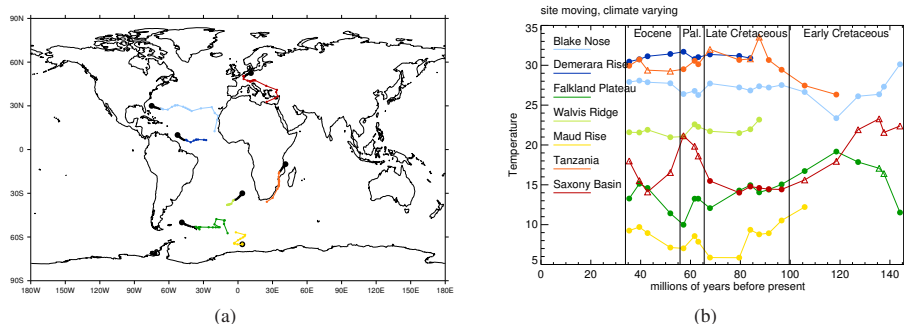


Figure 9. (a) The palaeolocation of 7 key sites used for reconstructing climate of the CPE. Large black dots represent the modern location. Small black dots represent the location at each Stage post the CPE, and coloured dots represent the location at each Stage during the CPE, for those Stages that the modern ocean crust was present. (b) Climate evolution across the CPE, simulated by the model, as experienced at the same 7 sites. Filled (open) symbols indicate that a particular site is marine (terrestrial) at a particular Stage.

Title Page

Abstract

Introduction

Conclusions

References

Tables

Figures



Back

Close

Full Screen / Esc

Printer-friendly Version

Interactive Discussion



Palaeogeographic controls on the climate system

D. J. Lunt et al.

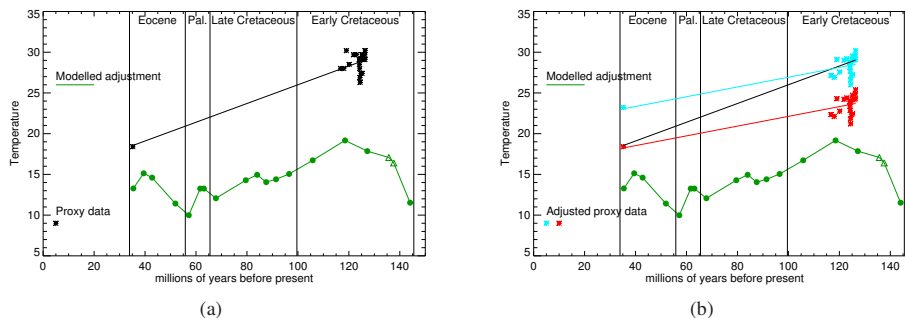


Figure 10. (a) Proxy temperature data (black asterixes) at Falkland plateau (Site 511) from TEX_{86} . Eocene data is from Liu et al. (2009), and Cretaceous data from Jenkyns et al. (2012). Black line shows the line of best fit. Also shown is the modelled temperature evolution at Falkland plateau (green line), i.e. the adjustment factor. In (b), the proxy data has been adjusted using the model output, relative to either the earliest (light blue) or latest (red) proxy data point.

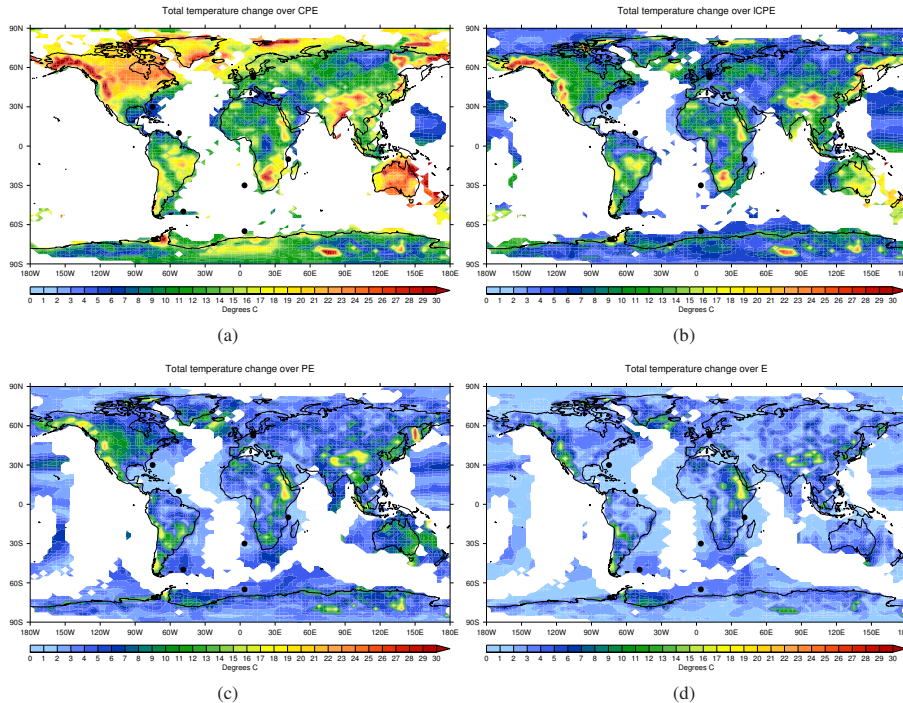


Figure 11. (a) Total temperature change across the CPE (maximum temperature in the CPE minus minimum temperature in the CPE, °C) for all modern locations, due to changes in palaeogeography and solar constant. Missing data (white) is where the Getech Plc plate model indicates that the modern location was not present across all the CPE. Also shown as black dots are the seven locations in Fig. 9. CPE is defined as from the early Cretaceous (Berriasian) to the late Eocene (Priabonian). (b–d) are similar, but show the change (b) from the late Cretaceous (Cenomanian) to the late Eocene (Priabonian), (c) from the early Paleocene (Danian) to the late Eocene (Priabonian), (d) from the early Eocene (Ypersian) to the late Eocene (Priabonian).